MODEL-BASED ULTRASONIC FLAW CLASSIFICATION AND SIZING

Lester W. Schmerr, Chien-Ping Chiou and Stephen M. Nugen

Center for NDE
Iowa State University
Department of Engineering Science and Mechanics
Ames, Iowa 50011

INTRODUCTION

The problem of flaw characterization can be viewed as a multi-step process (Fig. 1) where decisions are made as to flaw type (a classification process) and geometry (a sizing process). Previously, we have described our work on the use of the expert system FLEX for determining if an unknown flaw is a volumetric flaw or a crack [1] and the use of equivalent flaw sizing algorithms whereby the flaw is sized in terms of a best fit ellipsoid (for volumetric flaws) or ellipse (for cracks) [2]. Here, we will describe some of our work on how classification information can be used to improve sizing estimates and on the use of new, more efficient sizing algorithms.

SIZING AND CLASSIFICATION

Figure 1 describes an ultrasonic flaw characterization methodology in the form of a decision tree. In that tree, the flaw is first classified as to type. If the flaw is of a volumetric type (void or inclusion), the 1-D Inverse Born approximation is used to estimate the distance, D, from the center of the flaw to the front surface in the viewing direction (Fig. 2a). For a crack, the same distance is estimated by measuring the time separation between "flashpoints", i.e. when the incident wavefront strikes the front and back flaw edges (Fig. 2b). For either case, a single unified inversion algorithm then sizes the flaw in terms of an equivalent ellipsoid (volumetric case) or ellipse (crack case) that best matches the distances measured, at multiple viewing angles, in a least squares sense [2]. The classification step is essential in this method so that the data can be pre-processed appropriately (1-D Inverse Born or time between flashpoints) to extract the distance D.

Even if classification information is not available, it may be possible to extract D from the ultrasonic scattering data. Consider, for example, the ideal impulse response of a volumetric flaw and a crack in the Kirchhoff approximation as shown in Fig. 3a. In the volumetric case, the time domain response exhibits a large specular reflection followed by a step-like response, whereas in the crack case, we see two distinct antisymmetrical "flashpoints". Although these responses are quite different, if we integrate each response, the time, DT, between the first extremum of the signal and the first following zero can be used in both cases to estimate the distance D required in the sizing algorithm. In this case, a general ellipsoid is used to fit the data for both volumetric flaws and cracks.

Review of Progress in Quantitative Nondestructive Evaluation, Vol. 9
Edited by D.O. Thompson and D.E. Chimenti
Plenum Press, New York, 1990

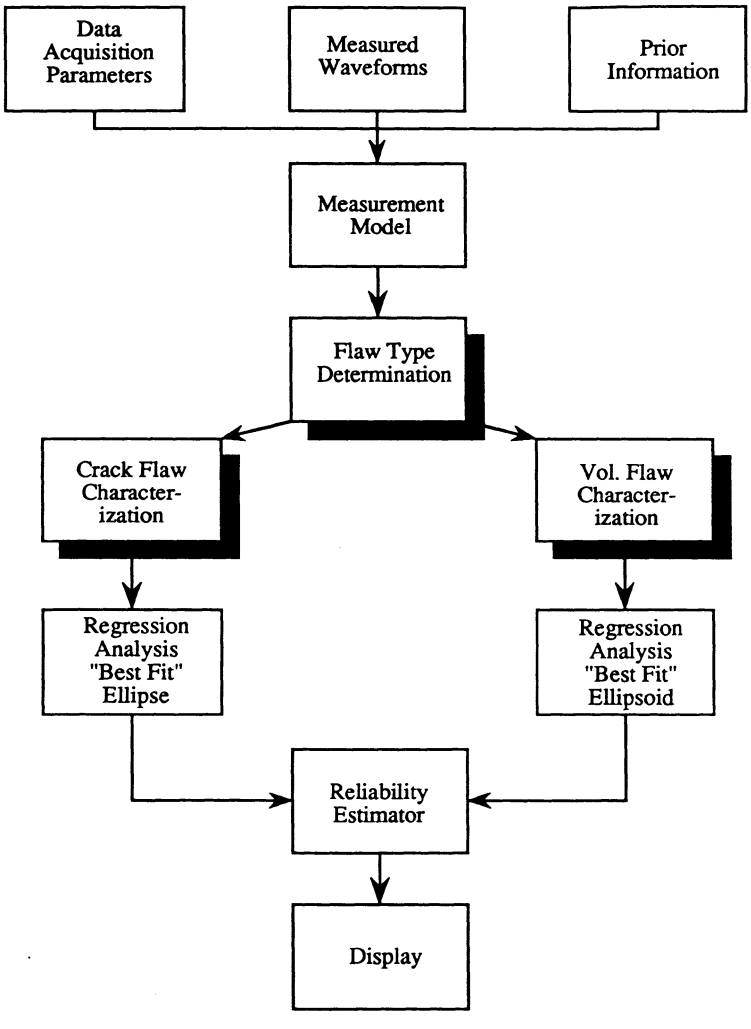

Fig. 1. Flaw Characterization Decision Tree

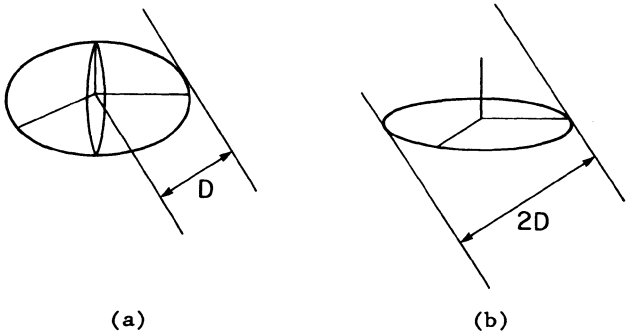

Fig. 2. Distance parameter D estimated for (a) a volumetric flaw, (b) a crack.

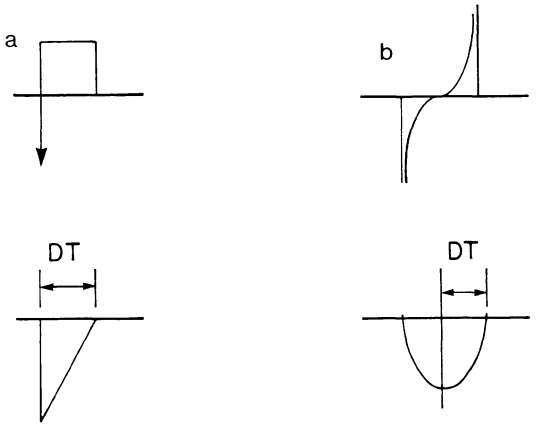

Fig. 3. (a) Impulse responses of an ellipsoidal void and elliptical flat crack in the Kirchhoff approximation. (b) Integrated impulse responses.

Table 1. Comparison of sizing of volumetric flaws and cracks with and without classification information. For the crack case ϕ_c is arbitrary since $\theta_c = 90°$.

	Case	Orientation Parameters (deg.)		Size Parameters (μm)		
		θ_c	ϕ_c	a	b	c
1.	Vol. with class	36	165	463	422	159
2.	without class	58	175	752	375	193
3.	exact	(60)	(180)	(400)	(400)	(200)
4.	Crack with class	92	---	423	389	0
5.	without class	102	---	411	321	97
6.	exact	(90)	(---)	(400)	(400)	(0)

Table 1 gives the results of sizing both a 400 x 400 x 200 μm spheroidal void and a 400 μm radius circular crack in titanium based on experimental data taken with a multiviewing transducer system [2,3]. For the volumetric flaw (cases 1-3), the use of classification information to allow the 1-D Inverse Born approximation to be used results in a reduction of the error in the largest size estimates from 88% to 16%. For the crack (cases 4-6) errors in the maximum size were reduced from 6% to 2.8%. Thus, classification information does also allow improved sizing, at least for the algorithms employed in this comparison.

In the crack case, the errors were able to be reduced to very small values by having classification information. This was possible because the knowledge that the flaw is a crack allows one to model, and hence remove, a consistent error present in the measurement process. To see this, recall that a flaw classified as a crack can be sized by merely measuring the time, 2DT, between "flashpoints". However, we have found that the finite bandwidth of any real system results in non-random DT measurement errors. By placing the same finite bandwidth restriction on the "ideal" waveforms predicted by the Kirchhoff approximation as shown in Fig. 3a, a "look-up" table can be constructed as shown in Fig. 4, to estimate this consistent error as a function of the measured time DT.

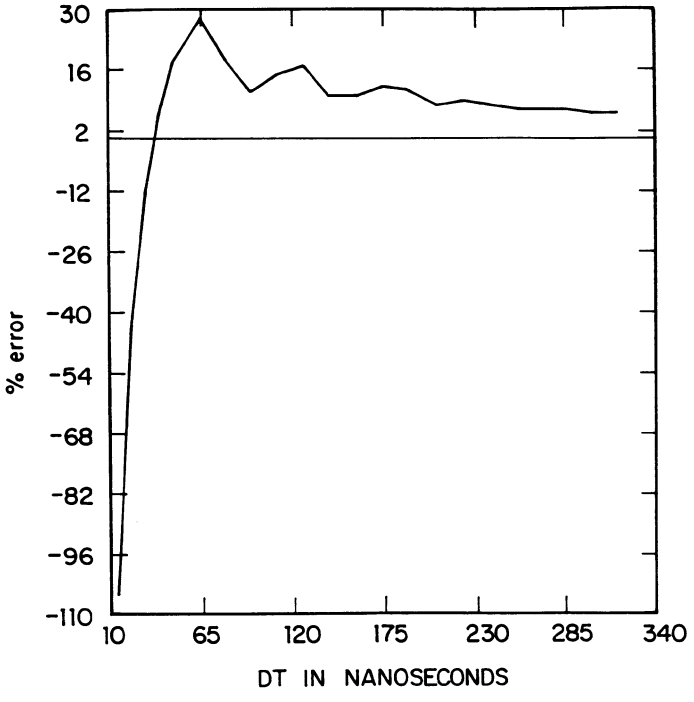

Fig. 4. Look-up table for the elimination of finite-bandwidth effects on time measurements DT.

For the crack example shown in Table 1, the crack parameters (θ_c,ϕ_c, a, b, c) would be estimated, using classification information and no DT corrections, as (93°, --, 374, 348, 0) resulting in a maximum sizing error of 6.5%, which is very similar to the results without classification. However, knowing the flaw is a crack and applying the corrections shown in Fig. 4 results in the size parameters shown in Table 1 (case 4) and reduces the maximum size errors to the 2.8% value mentioned previously.

A NEW SIZING METHOD

As the results of Table 1 demonstrate, the unified sizing algorithm can be used, with and without classification information, to provide reasonably accurate sizing based on experimental measurements of the DT parameter. Some of the disadvantages of this method are: a) it is iterative, leading at times to long computations b) it uses a non-linear least squares approach where convergence to the correct answer is difficult to guarantee, particularly in the case of noisy data and finally c) it is restricted to obtaining shape information only in terms of best-fit ellipsoids.

Recently, we have developed an alternate sizing algorithm that uses exactly the same scattering data but instead fits that data to a set of spherical harmonics with unknown coefficients. This new approach is non-iterative, leads to a linear least squares problem, and, in principle, is not restricted to simple shapes such as ellipsoids. The method works as follows. As mentioned previously, the measured times DT can be used to estimate the distance, D, between the center of the flaw and the front surface in a given viewing direction (Fig. 1). If we let

(θ_i, ϕ_i) be the angles which denote the ith viewing direction in a fixed spherical coordinate system, then $D_i = D(\theta_i, \phi_i)$ can be expanded in the form

$$D_i = \sum_m \sum_n C_{mn} f_{mn}(\theta_i, \phi_i) \qquad (i = 1, \ldots N) \tag{1}$$

where f_{mn} (θ_i, ϕ_i) are known spherical harmonic functions and C_{mn} are unknown coefficients. Using the expansion and the N measured values of D, D_{mi}, an error measure, E, can be formed as

$$E = \sum_{i=1}^{N} (D_i - D_{mi})^2 \tag{2}$$

Minimizing E then leads to a linear least squares problem for the determination of the C_{mn}. Once the C_{mn} are found, the value of $D(\theta, \phi)$ for any (θ, ϕ) is known. From this function the actual surface coordinates (x, y, z) of the flaw can be found via the relations [4]

$$x = D\sin\theta \cos\phi + \frac{\partial D}{\partial \theta} \cos\theta \cos\phi - \frac{\partial D}{\partial \phi} \frac{\sin\phi}{\sin\theta} \tag{3a}$$

$$y = D\sin\theta \sin\phi + \frac{\partial D}{\partial \theta} \cos\theta \, sm\phi + \frac{\partial D}{\partial \phi} \frac{\cos\phi}{\sin\theta} \tag{3a}$$

$$z = D\cos\theta - \frac{\partial D}{\partial \phi} \sin\theta \tag{3c}$$

Figure 5 shows a perspective view of the 400 x 400 x 200 μm spheroidal void in titanium that was used in our previous sizing/classification discussions. Applying the same measured data sets for this flaw to our new method and using only 9 terms in the expansion of eq. (1), a reconstructed shape was obtained as shown in Figure 6. Although the scales of Figs. 5 and 6 are somewhat different, comparison of two does show that the general flaw shape and orientation were captured quite well by the new algorithm. The size was also estimated well since along the (x, y, z) coordinate axes the exact flaw dimensions were (360, 400, 260) μm respectively, while in the reconstruction the corresponding values were (375, 497, 260) μm, leading to a maximum size error of

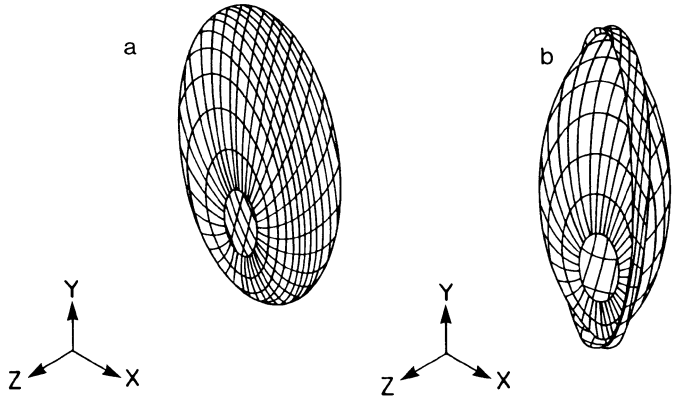

Fig. 5. (a) Geometry of a 400 x 400 x 200 μm spheroidal void. (b) Reconstructed geometry.

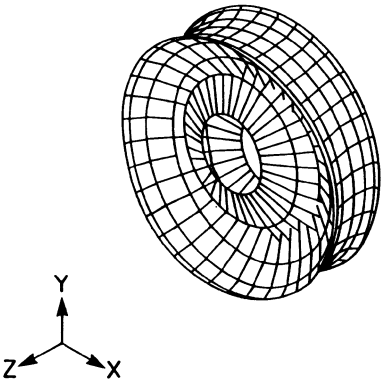

Fig. 6. Reconstructed geometry for a 400 μm radius circular crack in titanium.

approximately 24%, which is very comparable to that of the unified flaw sizing algorithm. We also applied this new method to the 400 μm crack considered previously. The results are given in Fig. 6. The reconstructed shape and orientation were both remarkably good considering the fact that spherical harmonic functions are not a good set of basis functions for reconstructing "disk"-like objects. The measured dimensions along the (x,y,z) axes were (512, 548, 160) μm, respectively, compared to the exact values of (400, 400, 0) μm. The error in the largest dimension was therefore, 37%. This result was not nearly as good as obtained by the unified sizing algorithm, but still quite acceptable we feel, given the limitations of the method for handling such singular geometries. (Note that the apparent "holes" shown in Figs. 5 & 6 are merely plotting artifacts and not real features.) We feel that the accuracy of this new sizing method is competitive with the unified sizing algorithm for volumetric flaws and still quite acceptable for cracks. Furthermore, it is fast because it is non-iterative, and stable. However, this new method is sensitive to data "outliers" since it, in effect, directly fits the data to the surface location. For cases such as shown above, where the average measurement errors are the order of 12%, the method performs well. Space does not permit us to illustrate the sensitivity of the method to large errors, but we can state that errors of 40-60% in single measurement values can cause the method to fail. In contrast, the unified sizing algorithm has been shown to be able to handle such "outliers" considerably better. This is to be expected since the constraint of fitting to a particular (ellipsoidal) shape causes large individual errors to be smeared out, leading to simply a degraded overall sizing estimate.

CONCLUSIONS

We have shown that classification information does improve flaw sizing estimates in two ways. First, it allows the use of what are currently the most robust equivalent flaw sizing algorithms that are available. Second, in the case of cracks, it allows systematic reduction of error in the measurements and hence improved results. We have also demonstrated a new sizing method that is non-iterative and linear in nature, that can be used as an alternate sizing method, with or without classification information, provided that large individual measurement errors are not present.

ACKNOWLEDGMENTS

We would especially like to thank Professors D. O. Thompson and D. K. Hsu and Mr. S. J. Wormley for supplying us with the experimental volumetric flaw data used here. Similarly, we thank Dr. T. A. Gray for the corresponding crack data. This research was supported by the Center for Nondestructive Evaluation at Iowa State University and was performed at Ames Laboratory. Ames Laboratory is operated for the U.S. Department of Energy by Iowa State University under Contract No. W-7405-ENG-82.

REFERENCES

1. Schmerr, L. W., Christensen, K. E., Nugen, S. M., Koo, L. S., and C. P. Chiou, "Ultrasonic Flaw Classification - An Expert System Approach," Review of Progress in Quantitative Nondestructive Evaluation, D. O. Thompson and D. E. Chimenti, eds, Vol. 8A, Plenum Press, New York, 657-664, 1989.
2. Schmerr, L. W., Sedov, A. and C. P. Chiou, "A Unified Constrained Inversion Model for Ultrasonic Flaw Sizing," Res. Nondestr. Eval., Vol. 1, 77-97, 1989.
3. Hsu, D. K. Thompson, D. O., and S. J. Wormley, "Reliability of Arbitrarily Oriented Flaws Using Multiview Transducer," IEEE Trans. Ultrasonics, Ferroelectrics and Frequency Control, Vol. UFFC-34, 508-514, 1987.
4. Borden, B., "A Vector Inverse Algorithm for Electromagnetic Scattering," SIAM J. Appl. Math, Vol. 44, 618-626, 1984.